Int. J. Heat Mass Transfer. Vol. 34, No. 12, pp. 3143–3150, 1991
Printed in Great Britain

0017–9310/91 $3.00 + 0.00

Numerical prediction of turbulent mixing in a variable-density swirling pipe flow

S. HIRAI and T. TAKAGI
Department of Mechanical Engineering, Faculty of Engineering, Osaka University, Suita, Osaka 565, Japan

(*Received* 11 *June* 1990 *and in final form* 7 *January* 1991)

Abstract—Numerical predictions are compared with experiments on turbulent mixing in variable density swirling flows, where He or CO_2 is coaxially injected in turbulent swirling air flows in a pipe. The calculation employs two kinds of stress/flux equation model, i.e. the density-weighted Favre-averaged form and the density-unweighted conventional-averaged form. The calculation based on the former model can predict the phenomenon that the mixing of He is strongly retarded due to swirl than that of CO_2, whereas the latter model fails to predict this. Comprehensible interpretations of the interrelation between turbulent mixing, density non-homogeneity and swirl-induced pressure gradient are presented.

1. INTRODUCTION

NUMERICAL calculation of turbulent swirling flow is of considerable importance for predicting flow, mixing and combustion in many furnaces and combustors with swirl. Swirling flow has been used to stabilize the flame and to obtain rapid combustion. The counter effect of the swirl, however, has been reported in the study of turbulent swirling flow in a circular tube with and without combustion [1, 2]. Turbulent mixing is retarded when swirl is introduced to the surrounding air flow in a confined tube.

The understanding of the effects of the swirl on the turbulent transport induced by the interaction of turbulence, swirl-induced pressure gradient and density nonhomogeneity is essential to control the mixing and combustion in swirling flows. It is also important to establish the prediction procedure of variable density turbulent swirling flow and mixing.

The previous reports by the authors pointed out that the k–ε two-equation model does not suffice but the stress/flux equation model [3, 4] has good performance on predicting characteristics of swirling flow and mixing [5, 6]. Superiority of the stress/flux equation model has been demonstrated in predicting laminarization phenomena [6] and the retardation of turbulent mixing [5] due to swirl. In the computation related to isothermal expanding swirling flow, Weber *et al.* [7] came to the conclusion that the stress model is far superior to the k–ε model. The stress/flux equation model has been found to be an effectual tool for the prediction of complex turbulent swirling flow and mixing.

In practical furnaces and combustors, density nonhomogeneity is caused by turbulent mixing and combustion. In the case of computations of turbulent flows which take the density fluctuation into consideration, turbulence models written in density-weighted time-averaged (Favre-averaged) form are much simpler than those in density-unweighted form [8]. Turbulence models with variable density and combustion are proposed and reported. These are illustrated in the reviews of Jones [8], Jones and Whitelaw [9], Libby and Williams [10] and Bilger [11]. Vandromme and Kollmann developed a density-weighted full second-order closure turbulence model and calculated free shear flows with mixing of gases with highly different density [12]. Janicka [13] and Dibble *et al.* [14] presented a second-order closure model for predicting diffusion flames. However, there have been no reports of applying the stress/flux equation model to turbulent swirling flow and mixing with significant density nonuniformity.

In the present study, computations are conducted on turbulent mixing in variable-density swirling flows in a stationary pipe. The constitution of the two types of stress/flux equation model, with and without considering density fluctuation, are illustrated in the first place. These models are employed in calculations and compared with experimental results of the turbulent mixing of helium (He) or carbon dioxide (CO_2) with air, with and without swirl [7]. Applicability of the turbulence models to the swirling and non-swirling flows are elucidated. Comprehensible interpretations of the interrelation between suppression and/or promotion of turbulent mixing, density nonhomogeneity and swirl-induced pressure gradient are presented.

2. BASIC EQUATIONS AND STRESS/FLUX EQUATION MODEL

The calculation is based on time-averaged conservation equations of mass, momentum and chemical species and transport equations of Reynolds stresses and turbulent fluxes of chemical species in an axisymmetric coordinate system, with and without swirl. Two types of time-averaged forms, density-weighted

NOMENCLATURE

C_S, C_1, C_2, C_c, C_{1c}, C'_{1c}, C_{2c}, $C_{\varepsilon 1}$, $C_{\varepsilon 2}$, $C_{\varepsilon 3}$, C_ε, C_{sm}, C_{pm} constants in stress/flux equation model
D_i diffusion term in scalar-flux equation model
k turbulent kinetic energy
M_l, m_l time-mean and fluctuating mass fraction of He or CO_2
p pressure
P_i production term in scalar-flux equation model
R_i pressure scrambling term in stress/flux equation model
U, V, W time-mean velocity components in the x-, r-, θ-directions
u, v, w fluctuating velocity components in the x-, r-, θ-directions
x, r coordinates
X axial distance from the nozzle tip.

Greek symbols
ε dissipation rate of k
ρ density.

Subscript
l chemical species l.

Superscripts
$\bar{}$ density-unweighted time averaging
$\tilde{}$ density-weighted time averaging.

and density-unweighted forms, are employed in the calculations. These are presented in the following sections.

2.1. *Basic equations and stress/flux equation model in density-weighted Favre-averaged form*

Conservation equations of mass, momentum and chemical species in density-weighted Favre-averaged form are shown in an axisymmetric cylindrical coordinate system applying the boundary layer approximation as follows:

$$\frac{\partial}{\partial x}(r\bar{\rho}\bar{U}) + \frac{\partial}{\partial r}(r\bar{\rho}\bar{V}) = 0 \tag{1}$$

$$\bar{\rho}\left(\bar{U}\frac{\partial \bar{U}}{\partial x} + \bar{V}\frac{\partial \bar{U}}{\partial r}\right) = -\frac{\partial \bar{p}}{\partial x} - \frac{1}{r}\frac{\partial}{\partial r}(r\bar{\rho}\,\overline{u''v''}) \tag{2}$$

$$\bar{\rho}\left(\bar{U}\frac{\partial \bar{W}}{\partial x} + \bar{V}\frac{\partial \bar{W}}{\partial r} + \frac{\bar{V}\bar{W}}{r}\right) = -\frac{1}{r^2}\frac{\partial}{\partial r}(r^2\bar{\rho}\,\overline{v''w''}) \tag{3}$$

$$\frac{\partial \bar{p}}{\partial r} = -\frac{\partial}{\partial r}\bar{\rho}\,\overline{v''^2} + \frac{\bar{\rho}}{r}(\bar{W}^2 + \overline{w''^2} - \overline{v''^2}) \tag{4}$$

$$\bar{\rho}\left(\bar{U}\frac{\partial \bar{M}_l}{\partial x} + \bar{V}\frac{\partial \bar{M}_l}{\partial r}\right) = -\frac{1}{r}\frac{\partial}{\partial r}(r\bar{\rho}\,\overline{v''m''_l}). \tag{5}$$

The double prime ($''$) designates the fluctuation with respect to the Favre-averaged quantity. u'', v'' and w'' are the fluctuation of velocity components with respect to the Favre-averaged axial, radial and tangential velocity $\bar{U}$, $\bar{V}$ and $\bar{W}$, respectively. Here ($\tilde{}$) and ($\bar{}$) indicate Favre average and conventional time average, respectively. m''_l is the fluctuation of mass fraction of chemical species l with respect to the Favre-averaged mass fraction of species $\bar{M}_l$. Transport of momentum or species by turbulent motion, represented by correlations between fluctuating velocities or fluctuating mass fraction and velocity in equations (2)–(5) is evaluated by the stress/flux equation model in the Favre-averaged form.

Density-weighted time-averaged transport equations for the correlation of the velocity fluctuations $\overline{\bar{\rho}u''_i u''_j}$ and for the correlation of velocity and mass fraction fluctuation $\overline{\bar{\rho}u''_i m''_l}$ can be written in a rectangular coordinate system, respectively, as follows:

$$\bar{\rho}\bar{u}_k\frac{\partial}{\partial x_k}\overline{\bar{\rho}u''_i u''_j} = \underbrace{-\overline{\bar{\rho}u''_j u''_k}\frac{\partial \bar{u}_i}{\partial x_k} - \overline{\bar{\rho}u''_i u''_k}\frac{\partial \bar{u}_j}{\partial x_k}}_{\text{(II)}}$$

$$\underbrace{-\frac{\partial}{\partial x_k}\{\overline{\bar{\rho}u''_i u''_j u''_k} + (\overline{p'u''_i}\delta_{jk} + \overline{p'u''_j}\delta_{ik}) - (\overline{u''_i\tau_{jk}} + \overline{u''_j\tau_{ik}})\}}_{\text{(III)}}$$

$$\underbrace{-\overline{u''_i}\frac{\partial \bar{p}}{\partial x_j} - \overline{u''_j}\frac{\partial \bar{p}}{\partial x_i}}_{\text{(IV)}} + \underbrace{\overline{p'\left(\frac{\partial u''_i}{\partial x_j} + \frac{\partial u''_j}{\partial x_i}\right)}}_{\text{(V)}} \underbrace{-\overline{\tau_{ik}\frac{\partial u''_j}{\partial x_k}} - \overline{\tau_{jk}\frac{\partial u''_i}{\partial x_k}}}_{\text{(VI)}} \tag{6}$$

$$\bar{\rho}\bar{u}_k\frac{\partial}{\partial x_k}\overline{\bar{\rho}u''_i m''_l} = \underbrace{-\overline{\bar{\rho}u''_k m''_l}\frac{\partial \bar{u}_i}{\partial x_k} - \overline{\bar{\rho}u''_k u''_i}\frac{\partial \bar{M}_l}{\partial x_k}}_{\text{(VIII)}}$$

$$\underbrace{-\frac{\partial}{\partial x_k}(\overline{\bar{\rho}u''_i u''_k m''_l} + \overline{m''_l p'}\delta_{ik})}_{\text{(IX)}}$$

$$\underbrace{\overline{p'\frac{\partial m''_l}{\partial x_i}}}_{\text{(X)}} \underbrace{-\overline{m''_l}\frac{\partial \bar{p}}{\partial x_i}}_{\text{(XI)}} \underbrace{-\left(\overline{\tau_{ik}\frac{\partial m''_l}{\partial x_k}} - \overline{j_{l,k}\frac{\partial u''_i}{\partial x_k}}\right)}_{\text{(XII)}} \tag{7}$$

where $\bar{u}_i$ and u''_i are the Favre-averaged velocity and velocity fluctuation in direction i, respectively.

Viscous stress and mass flux, are represented by τ_{ij} and $j_{l,k}$, respectively. In equations (6) and (7), terms (I) and (VII) (convection terms) and terms (II) and (VIII) (production terms) require no approximation. For term (III), the molecular diffusion term (con-

taining τ_{ij}) and the pressure-induced diffusion term (containing p') are negligible with respect to the diffusion by velocity fluctuation [3]. The contribution of the pressure fluctuation in term (IX) to the diffusion of species is negligible as compared with the third-order correlation [4]. The dissipative correlation term (XII) is zero with the assumption of isotropy of fine scale motion [4].

The remaining terms need to be approximated or modelled in terms of calculable flow properties. The turbulence models employed in the present calculations are rewritten from the constant density version of Daly and Harlow [15], Launder *et al.* [3] and Launder [4] for terms (III), (V), (IX) and (X), respectively, in terms of density-weighted averaged quantities as follows:

$$\frac{\partial}{\partial x_k}(\bar{\rho}\overline{\overline{u_i''u_j''u_k''}}) = -C_s\frac{\partial}{\partial x_k}\left(\bar{\rho}\frac{\bar{k}}{\bar{\varepsilon}}\overline{\overline{u_k''u_l''}}\frac{\partial\overline{\overline{u_i''u_j''}}}{\partial x_l}\right) \quad (8)$$

$$\begin{aligned}\overline{p'\left(\frac{\partial u_i''}{\partial x_j}+\frac{\partial u_j''}{\partial x_i}\right)} &= -C_1\bar{\rho}\frac{\bar{\varepsilon}}{\bar{k}}(\overline{\overline{u_i''u_j''}}-\tfrac{2}{3}\delta_{ij}\bar{k})\\ &+\frac{8+C_2}{11}\left(\bar{\rho}\overline{\overline{u_i''u_k''}}\frac{\partial\bar{u}_j}{\partial x_k}+\bar{\rho}\overline{\overline{u_j''u_k''}}\frac{\partial\bar{u}_i}{\partial x_k}\right)\\ &+\frac{8C_2-2}{11}\left(\bar{\rho}\overline{\overline{u_i''u_k''}}\frac{\partial\bar{u}_k}{\partial x_j}+\bar{\rho}\overline{\overline{u_j''u_k''}}\frac{\partial\bar{u}_k}{\partial x_i}\right)\\ &-\frac{30C_2-2}{55}\bar{\rho}\bar{k}\left(\frac{\partial\bar{u}_i}{\partial x_j}+\frac{\partial\bar{u}_j}{\partial x_i}\right)\\ &-\frac{6C_2+4}{11}\delta_{ij}\bar{\rho}\overline{\overline{u_l''u_k''}}\frac{\partial\bar{u}_l}{\partial x_k}\end{aligned} \quad (9)$$

$$\begin{aligned}\frac{\partial}{\partial x_k}(\bar{\rho}\overline{\overline{u_i''u_k''m_l''}}) &= -C_c\frac{\partial}{\partial x_k}\\ &\times\left\{\bar{\rho}\frac{\bar{k}}{\bar{\varepsilon}}\left(\overline{\overline{u_i''u_j''}}\frac{\partial\overline{\overline{u_k''m_l''}}}{\partial x_j}+\overline{\overline{u_k''u_j''}}\frac{\partial\overline{\overline{u_i''m_l''}}}{\partial x_j}\right)\right\}\end{aligned} \quad (10)$$

$$\begin{aligned}\overline{p'\frac{\partial m_l''}{\partial x_i}} &= -C_{1c}\frac{\bar{\rho}\bar{\varepsilon}}{\bar{k}}\overline{\overline{u_i''m_l''}}-C'_{1c}\frac{\bar{\rho}\bar{\varepsilon}}{\bar{k}}\\ &\times\left(\frac{\overline{\overline{u_i''u_j''}}}{\bar{k}}-\tfrac{2}{3}\delta_{ij}\right)\overline{\overline{u_j''m_l''}}+C_{2c}\bar{\rho}\overline{\overline{u_j''m_l''}}\frac{\partial\bar{u}_i}{\partial x_j}.\end{aligned} \quad (11)$$

Density–velocity covariance $\overline{u_i''}$ $(=-\overline{u_i'\rho'}/\bar{\rho})$ in term (IV) and density–concentration covariance $\overline{m_l''}$ $(=-\overline{m_l'\rho'}/\bar{\rho})$ in term (XI) are evaluated by the following relations:

$$\overline{u_i''} = -\overline{\overline{u_i''m_l''}}/\bar{\rho}\cdot\partial\bar{\rho}/\partial\bar{M}_l \quad (12)$$

$$\overline{m_l''} = -\overline{\overline{m_l''^2}}/\bar{\rho}\cdot\partial\bar{\rho}/\partial\bar{M}_l \quad (13)$$

where $\overline{\overline{m_l''^2}}$ in equation (13) is evaluated by the following transport equation [8]:

$$\begin{aligned}\bar{\rho}\bar{u}_k\frac{\partial\overline{\overline{m_l''^2}}}{\partial x_k} &= -2\bar{\rho}\overline{\overline{u_k''m_l''}}\frac{\partial\bar{M}_l}{\partial x_k}+C_{sm}\frac{\partial}{\partial x_k}\left(\bar{\rho}\frac{\bar{k}}{\bar{\varepsilon}}\overline{\overline{u_k''u_l''}}\frac{\partial\overline{\overline{m_l''^2}}}{\partial x_l}\right)\\ &-C_{pm}\bar{\rho}\frac{\bar{\varepsilon}}{\bar{k}}\overline{\overline{m_l''^2}}.\end{aligned} \quad (14)$$

Term (VI) in equation (6) has a character of dissipation, which can be written assuming the locally isotropic nature of the dissipative process as [12]

$$-\overline{\tau_{ik}\partial u_j''/\partial x_k}-\overline{\tau_{jk}\partial u_i''/\partial x_k} = -2/3\bar{\rho}\delta_{ij}\bar{\varepsilon}. \quad (15)$$

The dissipation rate of turbulent kinetic energy $\bar{\varepsilon}$ is evaluated by the following dissipation equation [8]:

$$\begin{aligned}\bar{\rho}\bar{u}_k\frac{\partial\bar{\varepsilon}}{\partial x_k} &= \frac{\partial}{\partial x_k}\left\{C_\varepsilon\frac{\bar{\rho}\bar{k}}{\bar{\varepsilon}}\overline{\overline{u_l''u_k''}}\frac{\partial\bar{\varepsilon}}{\partial x_l}\right\}\\ &+\frac{\bar{\rho}\bar{\varepsilon}}{\bar{k}}\left(-C_{\varepsilon1}\overline{\overline{u_l''u_k''}}\frac{\partial\bar{u}_l}{\partial x_k}-C_{\varepsilon2}\bar{\varepsilon}-C_{\varepsilon3}\frac{\overline{u_k''}}{\bar{\rho}}\frac{\partial\bar{p}}{\partial x_k}\right).\end{aligned} \quad (16)$$

The stress/flux equation model in the density-weighted averaged form contains empirical constants, which are adopted from refs. [3, 4, 8, 12, 15] as follows:

$$C_S = 0.22,\quad C_1 = 1.5,\quad C_2 = 0.4,\quad C_c = 0.11,$$
$$C_{1c} = 3.8,\quad C'_{1c} = -2.2,\quad C_{2c} = 0.33,\quad C_{\varepsilon1} = 1.45,$$
$$C_{\varepsilon2} = 1.90,\quad C_{\varepsilon3} = 2.0,\quad C_\varepsilon = 0.15,$$
$$C_{sm} = 0.11,\quad C_{pm} = 2.0.$$

Applying relations (8)–(11) and (13)–(15) to equations (6) and (7), the density-weighted correlations $\overline{\overline{u_i''u_j''}}$, $\bar{\varepsilon}$, $\overline{\overline{u_i''m_l''}}$ and $\overline{\overline{m_l''^2}}$ can be evaluated.

These correlations should be transformed in the axisymmetric cylindrical coordinate form in order to apply them to the calculation of flow and mixing in a circular pipe. The present calculation solves transport equations of ten correlations ($\overline{\overline{u''^2}}$, $\overline{\overline{v''^2}}$, $\overline{\overline{w''^2}}$, $\overline{\overline{u''v''}}$, $\overline{\overline{v''w''}}$, $\overline{\overline{u''w''}}$, $\overline{\overline{u''m_l''}}$, $\overline{\overline{v''m_l''}}$, $\overline{\overline{w''m_l''}}$, $\overline{\overline{m_l''^2}}$) and $\bar{\varepsilon}$ in an axisymmetric cylindrical coordinate system, applying the boundary layer approximation. For simplicity, only the transport equation of $\overline{\overline{v''m_l''}}$, which prescribes the species concentration, is shown below

$$\begin{aligned}&\bar{U}\frac{\partial\overline{\overline{v''m_l''}}}{\partial x}+\bar{V}\frac{\partial\overline{\overline{v''m_l''}}}{\partial r}-\overline{\overline{w''m_l''}}\frac{\bar{W}}{r}\\ &= -\left(\overline{\overline{v''^2}}\frac{\partial\bar{M}_l}{\partial r}-\overline{\overline{w''m_l''}}\frac{\bar{W}}{r}\right)-\overline{m_l''}\frac{\partial\bar{p}}{\partial r}\frac{1}{\bar{\rho}}\\ &-C_{1c}\frac{\bar{\varepsilon}}{\bar{k}}\overline{\overline{v''m_l''}}-C'_{1c}\frac{\bar{\varepsilon}}{\bar{k}}\left\{\frac{1}{\bar{k}}(\overline{\overline{v''^2}}\,\overline{\overline{v''m_l''}}\right.\\ &\left.+\overline{\overline{v''w''}}\,\overline{\overline{w''m_l''}}+\overline{\overline{u''v''}}\,\overline{\overline{u''m_l''}})-\tfrac{2}{3}\overline{\overline{v''m_l''}}\right\}\\ &-C_{2c}\overline{\overline{w''m_l''}}\frac{\bar{W}}{r}\\ &+2C_c\frac{1}{\bar{\rho}}\frac{\partial}{\partial r}\left\{\frac{\bar{\rho}\bar{k}}{\bar{\varepsilon}}\left(\overline{\overline{v''^2}}\frac{\partial\overline{\overline{v''m_l''}}}{\partial r}-\frac{\overline{\overline{v''w''}}\,\overline{\overline{w''m_l''}}}{r}\right)\right\}\\ &-2C_c\frac{1}{r^2}\frac{\bar{k}}{\bar{\varepsilon}}(\overline{\overline{w''^2}}\,\overline{\overline{v''m_l''}}+\overline{\overline{v''w''}}\,\overline{\overline{w''m_l''}})\\ &+2C_c\frac{1}{r}\frac{\bar{k}}{\bar{\varepsilon}}\left(\overline{\overline{v''^2}}\frac{\partial\overline{\overline{v''m_l''}}}{\partial r}-\overline{\overline{v''w''}}\frac{\partial\overline{\overline{w''m_l''}}}{\partial r}\right).\end{aligned} \quad (17)$$

2.2. *Basic equations and stress/flux equation model in density-unweighted conventional time-averaged form*

Basic equations and the stress/flux equation model in the density-unweighted conventional time-averaged form can be obtained by replacing ($''$) and ($\bar{}$) with ($'$) (conventional fluctuation) and ($\bar{}$), respectively, and by eliminating the terms including density fluctuation, $\overline{u_i''}$ and $\overline{m_i''}$. The transport equation for $\overline{\overline{m_i''^2}}$ need not be solved.

3. BOUNDARY CONDITION AND CALCULATION PROCEDURE

Boundary conditions are needed on the axis, near the wall region and at the inlet region. The present calculation employs the same conditions for the dependent variables in the density-weighted and density-unweighted equations, respectively. The boundary conditions near the wall and on the axis are the same as those mentioned in ref. [5]. The gradient of $\overline{\overline{m_i''^2}}$ is zero on the axis and near the wall.

Inlet conditions of calculations are determined on the cross section of the nozzle tip. Inlet conditions for the turbulent surrounding air are given as follows. The inlet profiles of $\bar{U}(=\tilde{U})$, $\bar{W}(=\tilde{W})$ and $\overline{u''^2}$ $(=\overline{u^2})$ are evaluated from the experimental values [17]. Flat profiles are given for inlet conditions of $\overline{v''^2}$ $(=\overline{v^2})$ and $\overline{w''^2}$ $(=\overline{w^2})$. The inlet profile of $\overline{u''v''}$ $(=\overline{uv})$ is evaluated from the transport equation of $\overline{u''v''}$ $(=\overline{uv})$ with the approximation of $\partial/\partial x \ll \partial/\partial r$, $\bar{V}(=\tilde{V})$ and of neglecting the diffusive transport. $\overline{v''w''}$ $(=\overline{vw})$ and $\overline{u''w''}$ $(=\overline{uw})$ are given by the linear profile connecting the boundary value near the wall with the zero value on the central axis. The dissipation rate $\bar{\varepsilon}(=\tilde{\varepsilon})$ is determined from the assumption of local equilibrium in the transport equation of turbulent kinetic energy $\bar{k}(=\tilde{k})$ employing the relation in the k–ε model. The values of $\overline{u''m_i''}$ $(=\overline{um_i})$, $\overline{v''m_i''}$ $(=\overline{vm_i})$, $\overline{w''m_i''}$ $(=\overline{wm_i})$ and $\overline{\overline{m_i''^2}}$ are zero.

The above differential equations are solved numerically using a finite difference method based on the procedure developed by Patankar and Spalding [16]. Seventy-four grid points are located in the radial direction with non-uniform intervals.

4. CALCULATION RESULTS AND DISCUSSION

The effects of swirl on the characteristics of variable density turbulent flow and mixing in a stationary pipe were studied experimentally in refs. [2, 7]. The flow configuration is shown in Fig. 1. Turbulent swirling or non-swirling air flow was formed in a pipe of 60 mm i.d. and He or CO_2, whose density is lighter or heavier than air, respectively, was coaxially injected from a round tube nozzle of 7 mm i.d. installed at the central axis. Radial profiles of axial and tangential velocity components are measured by a laser Doppler velocimeter (LDV) or a hot-wire probe. The concentration profiles of He and CO_2 were measured along the central axis. The concentration of He and CO_2 was analyzed by a gas chromatograph after gas sampling by a probe. It was noted that (1) the density non-homogeneity induced by He or CO_2 with air has a small influence on the time-mean velocity in both cases, with and without swirl, and (2) the characteristic difference of turbulent mixing is observed in the swirling flow condition, where the mixing of He is more strongly retarded than that of CO_2. In the non-swirling flow condition, however, the characteristic difference is not observed between the cases of He and CO_2.

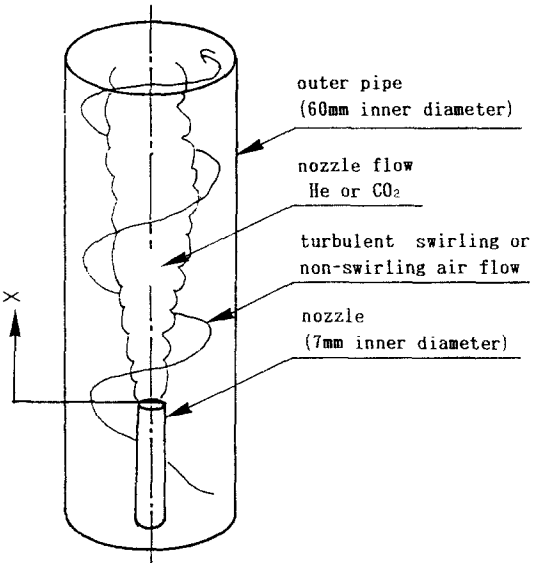

FIG. 1. Turbulent swirling flow configuration of calculation.

In the previous paper [5], numerical calculations were carried out employing the k–ε two-equation model and the stress/flux equation model, and were compared with the above-mentioned experiments in the flow region where the density nonuniformity is not significant. It was revealed that the calculation employing the stress/flux equation model can predict the characteristic flow field and retardation of mixing due to the swirl, whereas the k–ε two-equation model fails to predict this. In the present study, numerical computation is conducted and compared with the above-mentioned experiments in refs. [2, 17] including the flow region where the density nonuniformity is significant. Two kinds of transport equations are employed. One is the density-weighted Favre-averaged form and the other is the density-unweighted conventional time-averaged form. Hereafter, the calculation employing the conservation equations and the stress/flux equation model in the density-weighted time-averaged form is called Case A and that in the density-unweighted time-averaged form is called Case B.

In Fig. 2, the calculated velocity profiles at the cross section 300 mm downstream from the nozzle tip are compared with the experimental results [17] in the case of the swirling flow condition with He injected from the nozzle. The radial profiles of axial velocity

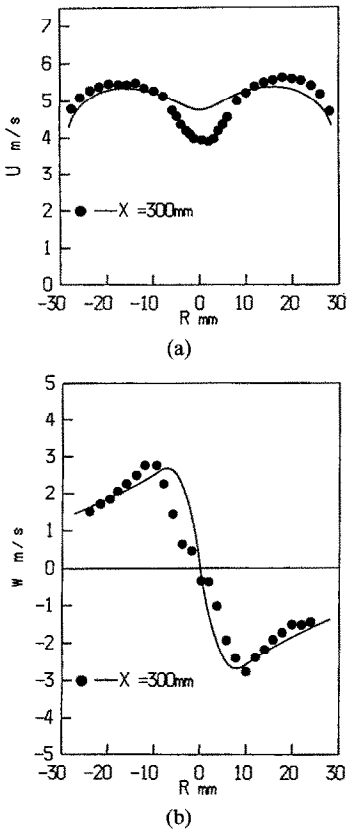

FIG. 2. Comparison of calculated and experimental radial profiles of axial and tangential velocity: (a) axial velocity profile; (b) tangential velocity profile.

U and tangential velocity W are shown in Figs. 2(a) and (b), respectively. Plotted points in Fig. 2 are experimental values by Yamada [17] and solid lines are the calculations. The distance from the central axis is denoted by R.

The measured axial velocity shows a depressed profile near the central axis, whereas the calculation estimates the velocity a little larger than the experiment alone. The overall agreement between the experimental and calculated axial velocity profiles, however, seems to be fairly good.

The measured tangential velocity shows a solid-rotational profile near the central axis and a free vortex profile at the outer region. The calculation can predict the experimental tendency.

In the case of CO_2, the characteristics between measured and predicted velocity profiles (U and W) show almost the same tendency presented in the case of He (Fig. 2).

In Fig. 3, the experimental and calculated profiles of He and CO_2 concentration along the central axis are compared in the non-swirling flow condition. Plotted points in Fig. 3 are experimental values from ref. [2]. The distance from the nozzle tip is denoted by X. The lines in Figs. 3(a) and (b) are the predicted ones employing the Favre-averaged type equations (Case A) and the conventional time-averaged ones (Case B), respectively. There is no noticeable difference between He and CO_2 experimental concentrations, which illustrates that the mixing characteristic of the lighter gas with air is the same with that of the heavier gas with air in the non-swirling flow. The calculations employing both the Favre-averaged type stress/flux equation model (Fig. 3(a)) and the conventional time-averaged one (Fig. 3(b)) can predict this experimental tendency of nearly the same concentration profiles of He and CO_2. In addition, the calculated profiles of Case A (Fig. 3(a)) and Case B (Fig. 3(b)) become similar for both cases of He and CO_2. $\widetilde{\overline{v''m_i''}}$ and $\overline{vm_i}$ predominately influence the concentration profiles of Case A and Case B, respectively. The crucial difference between the transport equations of $\widetilde{\overline{v''m_i''}}$ and $\overline{vm_i}$ is the term $-\overline{m_i''}\partial\bar{p}/\partial r/\bar{\rho}$ which is contained in Case A and not in Case B. The effect of the term $-\overline{m_i''}\partial\bar{p}/\partial r/\bar{\rho}$ on the concentration transport is negligible in the non-swirling flow due to the small radial pressure gradient $\partial\bar{p}/\partial r$ which is evaluated from equation (4).

In Fig. 4, the experimental and calculated concentration profiles of He and CO_2 along the central axis are compared in the swirling flow condition. Plotted points in Fig. 4 are experimental values from ref. [2]. The lines in Figs. 4(a) and (b) are the predicted ones employing the Favre-averaged type equations (Case A) and conventional time-averaged ones (Case B), respectively. The experimental results show that the concentration of He on the downstream axis is higher than that of CO_2, which indicates the turbulent mixing of low density gas in the central core with surrounding air is strongly retarded in the swirling flow than that of the high density gas. The calculation employing the Favre-averaged type equations (Case A) can predict well the experimental tendency, the characteristic difference between the turbulent mixing of He and CO_2 due to the swirl (Fig. 4(a)). The calculation employing the conventional time-averaged type equations (case B), however, fails to predict the experimental results (Fig. 4(b)). The calculated concentration of He and CO_2 along the central axis shows nearly the same profile in Case B. Thus, the computation of Case A which takes the density fluctuation into account can predict the phenomenon that the mixing of He with air is significantly more suppressed than that of CO_2.

The success of the computation employing the Favre-averaged equations is considered to be caused by the fact that the radial turbulent transport of He is estimated smaller than that of CO_2.

This phenomenon can be investigated by comparing the characteristics of the terms in the transport equation of turbulent radial flux of species $\widetilde{\overline{v''m_i''}}$ in cases of He and CO_2. The radial profile of the terms in the transport equation (17) of $\widetilde{\overline{v''m_i''}}$ at the cross section of $XD = 100$ mm are indicated in Fig. 5. Figures 5(a) and (b) are the cases of He and CO_2, respectively. The marks in the figure P_i, R_i, D_i ($i = 1, 2, 3$) indicate the terms in equation (17).

P_i ($i = 1, 2, 3$) are the production terms. P_1

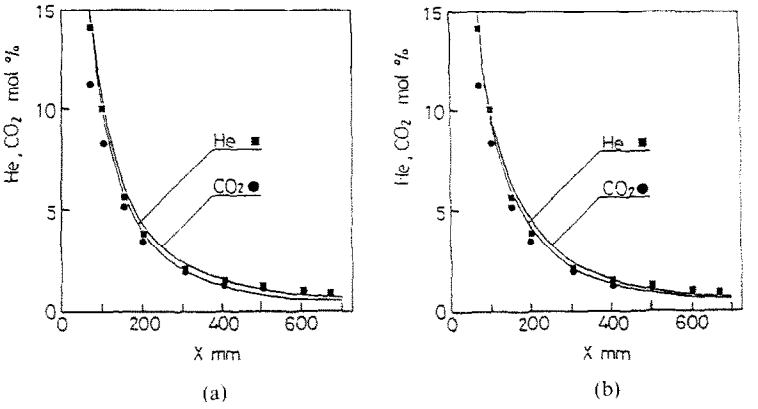

FIG. 3. Comparison of calculated and experimental concentration of He and CO_2 along the central axis in non-swirling flow condition: (a) predictions applying Favre-averaged form; (b) predictions applying conventional time-averaged form.

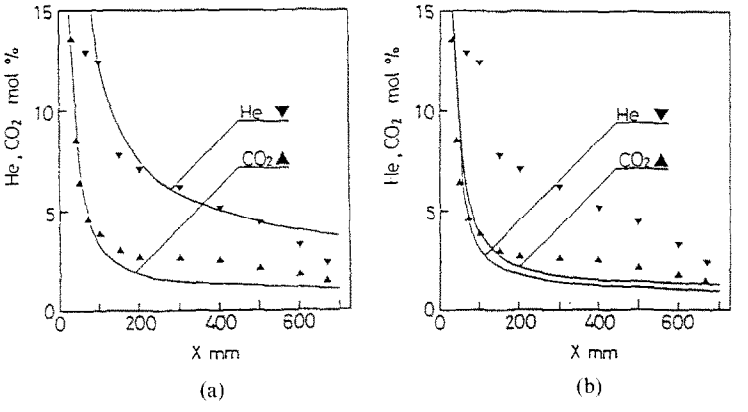

FIG. 4. Comparison of calculated and experimental concentration of He and CO_2 along the central axis in swirling flow condition: (a) predictions applying Favre-averaged form; (b) predictions applying conventional time-averaged form.

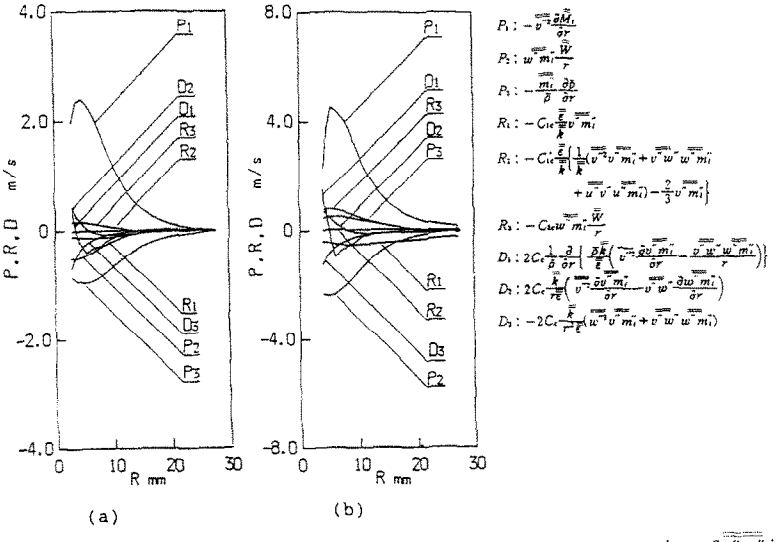

FIG. 5. Calculated radial profiles of the magnitude of the terms in the transport equation of $\overline{\overline{\rho v'' m_i''}}$ in swirling flow: (a) calculation in the case of He; (b) calculation in the case of CO_2.

$(= -\overline{\overline{v''^2}}\,\partial\bar{M}_l/\partial r)$ is exclusively concerned with the radial gradients of time-mean concentrations of He and CO_2 and becomes positive in both cases of He and CO_2. P_1 contributes significantly to the production of $\overline{\overline{v''m_l''}}$. P_1 causes the concentration of He and CO_2 to diffuse in the radial direction. P_2 $(=\overline{\overline{w''m_l''}}\,\bar{W}/r)$, including tangential velocity $\bar{W}$, becomes a negative production term which reduces the magnitude of $\overline{\overline{v''m_l''}}$ and retards the turbulent transport due to swirl in both cases of He and CO_2.

P_3 $(= -\overline{m_l''}/\bar{\rho}\,\partial\bar{p}/\partial r)$ consists of the term $\overline{m_l''}$ $(= -\overline{m'\rho'}/\bar{\rho})$ arising from the density fluctuation and the radial pressure gradient $\partial\bar{p}/\partial r$. P_3 has the opposite sign between the cases of He and CO_2.

In the case of He, P_3 $(= -\overline{m_l''}/\bar{\rho}\partial\bar{p}/\partial r)$ becomes a negative production term and has a significant effect on the retardation of turbulent mixing. P_3 $(= -\overline{m_l''}/\bar{\rho}\partial\bar{p}/\partial r)$ has a comparable magnitude as compared with other production terms P_1 or P_2. Contrary to the case of He, P_3 $(= -\overline{m_l''}/\bar{\rho}\partial\bar{p}/\partial r)$ becomes a positive production term in the case of CO_2 and promotes turbulent mixing, but its magnitude is small as compared with other production terms P_1 or P_2.

The contradictory effect of P_3 between the cases of He and CO_2 is caused by the sign of $\overline{m_l''}$ evaluated from equation (13), where $\partial\bar{\rho}/\partial\bar{M}_l$ becomes minus in the case of He and plus in the case of CO_2.

The reason why P_3 has a significant effect in the case of He and not in the case of CO_2 is caused by the magnitude of $\partial\bar{\rho}/\partial\bar{M}_l$, where the absolute value of $\partial\bar{\rho}/\partial\bar{M}_l$ is large in the case of He and not in the case of CO_2. The absolute magnitude of $\partial\bar{\rho}/\partial\bar{M}_l$ is strongly related to the density ratio between the nozzle fluid (He or CO_2) and surrounding fluid (air).

Other terms R_i and D_i $(i = 1, 2, 3)$ show nearly the same characteristics for the cases of He and CO_2. Thus the calculated difference of concentration between He and CO_2 in the swirling flow is caused by the production term P_3 $(= -\overline{m_l''}/\bar{\rho}\partial\bar{p}/\partial r)$ in the $\overline{\overline{v''m_l''}}$ transport equation of He. The significant effect of P_3 $(= -\overline{m_l''}/\bar{\rho}\partial\bar{p}/\partial r)$ in the case of He arises from the strong density fluctuation $\overline{m_l}$ $(= -\overline{m'\rho'}/\bar{\rho})$ caused by the mixing between highly different density fluids and large radial pressure gradient $\partial\bar{p}/\partial r$ evaluated from equation (4) due to the swirl velocity. The term P_3 is not included in the density-unweighted conventional time-averaged type stress/flux equation model, in which density fluctuation is not considered.

5. CONCLUSION

Computations on variable density turbulent pipe flow and mixing with and without swirl were conducted in order to investigate the applicability of the turbulence models and to reveal the mechanism of the swirl-induced turbulent mixing with significant density nonhomogeneity. The present calculation employs two stress/flux equation turbulence models with and without considering density fluctuation written in the density-weighted Favre-averaged form and density-unweighted conventional time-averaged form. The computations were compared with the experiments on the turbulent mixing of He or CO_2 with air in swirling and non-swirling flows. The results obtained are as follows.

(1) In the non-swirling flow, calculations employing both the Favre-averaged and the conventional-averaged stress flux equation models can predict the experimental mixing characteristics where the concentration profiles of He and CO_2 are nearly the same. There is a small difference between the calculated concentration of the two models. The reason is that the effect of the term $-\overline{m_l''}/\bar{\rho}\partial\bar{p}/\partial r$, included in the Favre-averaged $\overline{\overline{v''m_l''}}$ equation is small due to the small radial pressure gradient in the non-swirling flow.

(2) The computations employing the stress/flux equation model in the density-weighted Favre-averaged form can predict the characteristic difference of the turbulent mixing of He or CO_2 with air. The mixing of He is more strongly retarded than that of CO_2. The computation employing the stress/flux equation model in density-unweighted conventional time-averaged form, however, fails to predict the phenomena. The success of the prediction applying the density-weighted stress/flux equation model comes from the inclusion of the production term $-\overline{m_l''}/\bar{\rho}\,\partial\bar{p}/\partial r$, which consists of the term including the density fluctuation and the large radial pressure gradient due to the swirl in the transport equation of $\overline{\overline{v''m_l''}}$. This production term plays an important role on the turbulent transport of species in variable-density turbulent swirling flows.

REFERENCES

1. T. Takagi, T. Okamoto, M. Taji and Y. Nakasuji, Retardation of mixing and counter-gradient diffusion in a swirling flame, *Twentieth Symp. (Int.) on Combustion*, pp. 251–258. Combustion Institute, Pittsburgh, Pennsylvania (1984).
2. T. Takagi, T. Okamoto and M. Yamada, Phenomena of the retardation of mixing and combustion in swirling flows, *Proc. ASME/ JSME Thermal Engng Joint Conf.*, Vol. 4, pp. 131–136 (1983).
3. B. E. Launder, G. J. Reece and W. Rodi, Progress in the development of a Reynolds-stress turbulence closure, *J. Fluid Mech.* **88,** 537–566 (1975).
4. B. E. Launder, *Turbulence* (Edited by P. Bradshaw), pp. 232–289. Springer, Berlin (1976).
5. S. Hirai, T. Takagi and T. Higashiya, Numerical prediction of flow characteristics and retardation of mixing in a turbulent swirling flow, *Int. J. Heat Mass Transfer* **32,** 121–130 (1989).
6. S. Hirai, T. Takagi and M. Matsumoto, Predictions of the laminarization phenomena in an axially rotating pipe flow, *Trans. ASME, J. Fluids Engng* **110,** 424–430 (1988).
7. R. Weber, F. Boysan, J. Swithenbank and P. A. Roberts, Computations of near field aerodynamics of swirling expanding flows, *Twenty-first Symp. (Int.) on Combustion*, pp. 1435–1443. Combustion Institute, Pittsburgh, Pennsylvania (1986).
8. W. P. Jones, *Prediction Methods for Turbulent Flows* (Edited by W. Kollmann), pp. 379–422. Hemisphere, Washington, DC (1980).
9. W. P. Jones and J. H. Whitelaw, Calculation methods

for reacting turbulent flows, a review, *Combust. Flame* **48,** 1–26 (1982).
10. A. Libby and F. A. Williams, Turbulent reacting flows. In *Topics in Applied Physics*, Vol. 4. Springer, Berlin (1980).
11. R. W. Bilger, Turbulent diffusion flames, *Ann. Rev. Fluid Mech.* **21,** 101–135 (1989).
12. D. Vandromme and W. Kollmann, Second order closure for variable density free shear layer, *Turbulent Shear Flow* **3,** 275–290 (1981).
13. J. Janicka, A Reynolds-stress model for the prediction of diffusion flame, *Twenty-first Symp. (Int.) on Combustion*, pp. 1409–1417 (1986).
14. R. W. Dibble, W. Kollmann, M. Farshchi and R. W. Schefer, Second-order closure for turbulent nonpremixed flames: scaler dissipation and heat release effects, *Twenty-first Symp. (Int.) on Combustion*, pp. 1329–1340. Combustion Institute, Pittsburgh, Pennsylvania (1986).
15. B. J. Daly and F. H. Harlow, Transport equations in turbulence, *Physics Fluids* **13,** 2634 2649 (1970).
16. S. V. Patankar and D. B. Spalding, *Heat and Mass Transfer in Boundary Layers*, pp. 28–46. Intertext (1970).
17. M. Yamada, The study of mixing and combustion in swirling flows, Master's Thesis, Osaka University (1982).

PREDICTION NUMERIQUE DU MELANGEAGE TURBULENT DANS UN ECOULEMENT TOURNANT DANS UN TUBE AVEC DENSITE VARIABLE

Résumé—Des prédictions numériques sont comparées avec des expériences sur le mélangeage turbulent dans un écoulement tournant à densité variable, où He ou CO_2 est coaxialement injecté dans un écoulement d'air à vortex turbulent. Le calcul utilise deux sortes de modèle à contrainte/flux: la forme de moyenne selon Favre pondérée par la densité et la forme de moyenne habituelle non pondérée. Le calcul basé sur le premier modèle peut prédire le fait que le mélangeage de He est fortement retardé par le tourbillon par rapport au cas du CO_2. Par contre le dernier modèle ne le peut pas. On présente des interprétations compréhensibles de l'interaction entre le mélangeage turbulent, la non homogénéité de la densité et le gradient de pression induite par le tourbillon.

NUMERISCHE BERECHNUNG DER TURBULENTEN MISCHUNG IN EINER VERWIRBELTEN ROHRSTRÖMUNG MIT VARIABLER DICHTE

Zusammenfassung—Die turbulenten Mischungsvorgänge zwischen einer turbulenten verwirbelten Luftströmung in einem Rohr und einer axialen Einblasung von He oder CO_2 werden numerisch berechnet und mit Versuchsdaten verglichen. Bei den Berechnungen werden zwei unterschiedliche Arten der "streß/flux"-Gleichung verwendet: einerseits die Form mit Dichtegewichtung und Mittelwertbindung nach Favre, andererseits die Form ohne Dichtegewichtung mit herkömmlicher Mittelwertbindung. Die Berechnung nach dem ersten Modell erlaubt die Vorhersage des Phänomens, daß die Mischung von He im Vergleich zu CO_2 aufgrund der Verwirbelung stark verzögert ist. Das zweite Modell versagt in dieser Hinsicht. Abschließend werden verständliche Interpretationen für die Wechselbeziehung zwischen turbulenter Vermischung, Inhomogenität der Dichte und durch die Verwirbelung verursachte Druckgradienten angegeben.

ЧИСЛЕННОЕ ОПРЕДЕЛЕНИЕ ТУРБУЛЕНТНОГО СМЕШЕНИЯ В ЗАКРУЧЕННОМ ТЕЧЕНИИ С ПЕРЕМЕННОЙ ПЛОТНОСЛЬЮ В ТРУБЕ

Аннотация—Проводится сравнение численных расчетов с экспериментальными данными по турбулентному смешению в закрученных течениях с переменной плотностью в трубе в случаях, когда в указанное течение тангенциально вводятся He или CO_2. В расчетах используются два вида модельной зависимости между напряжением и потоком, а именно, усреднение по фавру со взвешенной плотностью и обычное усреднение с невзвешенной плотностью. Расчет на основе первой модели обнаружил, что смешение He является существенно замедленным мз-за наличия закрутки по сравнению с CO_2, в то время как вторая модель не приводит к такому выволу. Объясняется взаимосвязь между турбулентным смешением, неоднородностью плотности и градиентом давления, вызванным закруткой.